

Sponge contribution to the silicon cycle of a diatom-rich shallow bay

María López-Acosta ^{1,2*} Manuel Maldonado ³ Jacques Grall ⁴ Axel Ehrhold ⁵ Cèlia Sitjà ³
Cristina Galobart ³ Fiz F. Pérez ¹ Aude Leynaert ²

¹Instituto de Investigaciones Marinas (IIM), CSIC, Vigo, Spain

²Laboratoire des Sciences de l'Environnement Marin, UMR 6539, Institut Universitaire Européen de la Mer, Plouzané, France

³Centro de Estudios Avanzados de Blanes (CEAB), CSIC, Girona, Spain

⁴Observatoire des Sciences de l'Univers, UMS 3113, Institut Universitaire Européen de la Mer, Plouzané, France

⁵IFREMER, Géosciences Marines, Centre de Brest, Plouzané, France

Abstract

In coastal systems, planktonic and benthic silicifiers compete for the pool of dissolved silicon, a nutrient required to make their skeletons. The contribution of planktonic diatoms to the silicon cycle in coastal systems is often well characterized, while that of benthic silicifiers such as sponges has rarely been quantified. Herein, silicon fluxes and stocks are quantified for the sponge fauna in the benthic communities of the Bay of Brest (France). A total of 45 siliceous sponge species living in the Bay account for a silicon standing stock of 1215 tons, while that of diatoms is only 27 tons. The silicon reservoir accumulated as sponge skeletons in the surface sediments of the Bay rises to 1775 tons, while that of diatom skeletons is only 248 tons. These comparatively large stocks of sponge silicon were estimated to cycle two orders of magnitude slower than the diatom stocks. Sponge silicon stocks need years to decades to be renewed, while diatom turnover lasts only days. Although the sponge monitoring over the last 6 yr indicates no major changes of the sponge stocks, our results do not allow us to conclude if the silicon sponge budget of the Bay is at steady state, and potential scenarios are discussed. The findings buttress the idea that sponges and diatoms play contrasting roles in the marine silicon cycle. The budgets of these two major silicon users need to be integrated and their connections revealed, if we aim to improve our understanding of the silicon cycling in coastal ecosystems.

There is great interest in understanding the cycling of silicon (Si) in marine environments because this nutrient is key to the functioning of marine ecosystems. In coastal oceans, Si is responsible for sustaining a large proportion of primary

productivity and many of the food webs that ultimately sustain fish and human populations (Kristiansen and Hoell 2002; Ragueneau et al. 2006). Shortage of Si availability in coastal areas frequently reflects situations of ecosystem disequilibrium and proliferation of harmful algal blooms (Davidson et al. 2014; Glibert and Burford 2017; Thorel et al. 2017). Thus, a thorough understanding of the cycling of Si in coastal marine environments is critical for effective ecosystem management.

A substantial part of the Si cycling in the marine environment occurs through a variety of microorganism and macroorganism, the silicifiers, which require Si to build their skeletons. The silicifiers, which include diatoms, silicoflagellates, most species of sponges and rhizarians, and several species of choanoflagellates, consume dissolved Si from seawater to build their skeletons made of biogenic silica (i.e., SiO₂; hereafter referred as biogenic Si). After death, their siliceous skeletons get partially dissolved as they sink and in marine sediments as they are buried. This dissolved silica feeds the pool of dissolved Si that is biologically available for silicifiers and facilitates the recycling of this nutrient (DeMaster 2003; Tréguer et al. 2021). To date, our understanding of

*Correspondence: lopezacosta@iim.csic.es

This is an open access article under the terms of the [Creative Commons Attribution-NonCommercial](https://creativecommons.org/licenses/by-nc/4.0/) License, which permits use, distribution and reproduction in any medium, provided the original work is properly cited and is not used for commercial purposes.

Additional Supporting Information may be found in the online version of this article.

Author Contribution Statement: M.L.A. and M.M. conceived and designed the study. M.L.A. conducted the sponge fieldwork, with the help of J.G. and A.L. M.L.A., M.M., and C.S. taxonomically identified the sponges. M.L.A. processed the sponge samples to determine specific silica content. A.E. sampled the sediment cores and provided sedimentary data. J.G. and A.E. provided the bottom mapping data and M.L.A. developed the benthic habitat and spicule accumulation layers. M.L.A., C.G., and C.S. conducted sponge silica determination under the microscope. M.L.A. analyzed and interpreted the data and drafted the manuscript, with invaluable inputs made by M.M. and A.L. All authors contributed with comments to the manuscript and approved the submitted version. M.L.A., J.G., F.F.P., and M.M. acquired the funding and administrated the projects leading to this publication.

the biogeochemical cycling of Si in the marine environment is based predominantly on the role of diatoms, microscopic unicellular eukaryotic algae which are the most abundant silicifiers in the global ocean (Malviya et al. 2016; Tréguer et al. 2021). Recently, some studies have revealed that other silicifiers such as siliceous Rhizaria and sponges also contribute significantly to the marine Si cycle at local and global scales (Biard et al. 2018; Maldonado et al. 2019; Llopis Monferrer et al. 2020). However, the contribution of these organisms to the Si cycle often has large uncertainties associated which need to be addressed at the regional scale (Tréguer et al. 2021). To quantify the cycle contribution of siliceous sponges is particularly complicated given their benthic nature and heterogeneous distribution across the depths of the world's oceans. However, there is growing evidence that sponges are important contributors to the Si cycle in terms of Si standing stocks and reservoirs (Maldonado et al. 2010, 2019).

In the present study, the Bay of Brest (France) was monitored to assess the relative contribution of siliceous sponges to the Si budget of this emblematic coastal system. This Bay has been the subject of numerous ecological, biogeochemical, and physical studies and is currently one of the best-studied coastal ecosystems in Europe, in terms of both structure and ecosystem functioning (Le Pape et al. 1996; Del Amo et al. 1997; Ragueneau et al. 2018). In this ecosystem, diatoms dominate the annual pelagic primary production (Quéguiner and Tréguer 1984; Del Amo et al. 1997). Other planktonic silicifiers such as silicoflagellates, polycystines, and phaeodarians are rarely recorded in the monthly surveys of the planktonic community of the Bay, and when found, they are low abundant (<https://www.phytobs.fr/>). Dissolved Si concentrations vary over the yr cycle from below 1 μM in spring and early summer up to 15–20 μM in late autumn and winter. Therefore, in this ecosystem, diatom activity is limited by dissolved Si principally during spring and early summer (Ragueneau et al. 2002), but sponges are limited all yr round, as these organisms need dissolved Si concentrations of 100–200 μM to reach their maximum speed of Si consumption ($K_M = 30\text{--}100 \mu\text{M Si}$; López-Acosta et al. 2016, 2018).

In this system, both dredging and diving research activities have identified important populations of siliceous sponges (Jean 1994; López-Acosta et al. 2018), and a previous study firstly estimated that the sponge silica production represents ca. 8% of the net annual silica production in the Bay (López-Acosta et al. 2018). Nevertheless, the large amounts of Si within the sponge bodies (i.e., the Si standing stock) remain unquantified and the fate of such Si once the sponges die. Herein, we estimate these parameters and provide the most complete cycle of Si through sponges for this coastal ecosystem. The findings are discussed within the regional Si budget of the Bay of Brest previously published by Ragueneau et al. (2005), which considered only the contribution of planktonic diatoms.

Materials

Study area

The Bay of Brest (NW France) is a semi-enclosed marine ecosystem of about 130 km² (harbors and estuaries not included) that is connected to the Atlantic Ocean through a narrow (1.8 km wide) and deep (45 m) strait. The Bay is a shallow system, with a maximum depth of 40 m and a mean depth of 8 m. It is a macrotidal (maximum tidal amplitude = 8 m) system that receives high-nutrient loadings mainly from two small rivers (Fig. 1a). All yr round, the tidal and wind currents, together with the shallowness of the Bay, cause the nutrient concentration to remain relatively homogeneous in the water column (Delmas and Tréguer 1985; Salomon and Breton 1991; Le Pape et al. 1996).

The Bay hosts abundant and diverse benthic communities, developed in a mixture of hard and soft substrates (Grall and Glémarec 1997). The benthic ecosystem of the Bay consist of six major habitats, according to depth, nature of substrate, and biota (Hily et al. 1992; Gregoire et al. 2016): (1) the rocky intertidal coastline that remains emerged during spring low tides; (2) the rocky subtidal bottoms, down to 20 m depth, that mostly surround the islets of the Bay; (3) the maerl beds, soft bottoms with dense assemblages of *Lithothamnion corallioides*, together with some *Phymatolithon calcareum* and *Lithophyllum* cf. *fasciculatum*, down to 15 m depth; (4) the shallow mud bottoms down to 10 m depth, mostly in the peripheral zones of the Bay; (5) the heterogeneous sediments from 5 to 25 m depth which consist of a mix of mud, calcareous detritus, and gravel bottoms; and (6) the circalittoral coarse sediments, consisting of gravel and pebble bottoms located mostly in the central, deepest zones (20–40 m) of the Bay (Fig. 1a–g). Using QGIS software, version 3.10.2 (QGIS Development Team 2020), the benthic habitats of the Bay were delimited and their areas were calculated (Fig. 1a; Table 1). This resulted in the most updated map of the benthic habitats of the Bay of Brest (López-Acosta 2022), which includes the up-to-date information of the bottom communities of the Bay from the annual monitoring conducted by the Marine Observatory of the European Institute for Marine Studies (Derrien-Courtet et al. 2019).

Silicon standing stock in sponge communities

To estimate the Si standing stock of the sponge communities within the Bay of Brest, quantitative surveys were conducted across the six benthic habitats. The sampling effort carried out within a given habitat depended on both its relative surface to the total Bay extension and the relative internal variation (Eberhardt 1978). Three sampling techniques were used for the different habitats: (1) the rocky intertidal was sampled by using 23 random quadrats (1 × 1 m) at low tides; (2) the rocky subtidal, the maerl beds, the shallow mud, and the heterogeneous sediments above 20 m depth were sampled by scuba diving using 119 random 1 × 1 m quadrats; (3) the

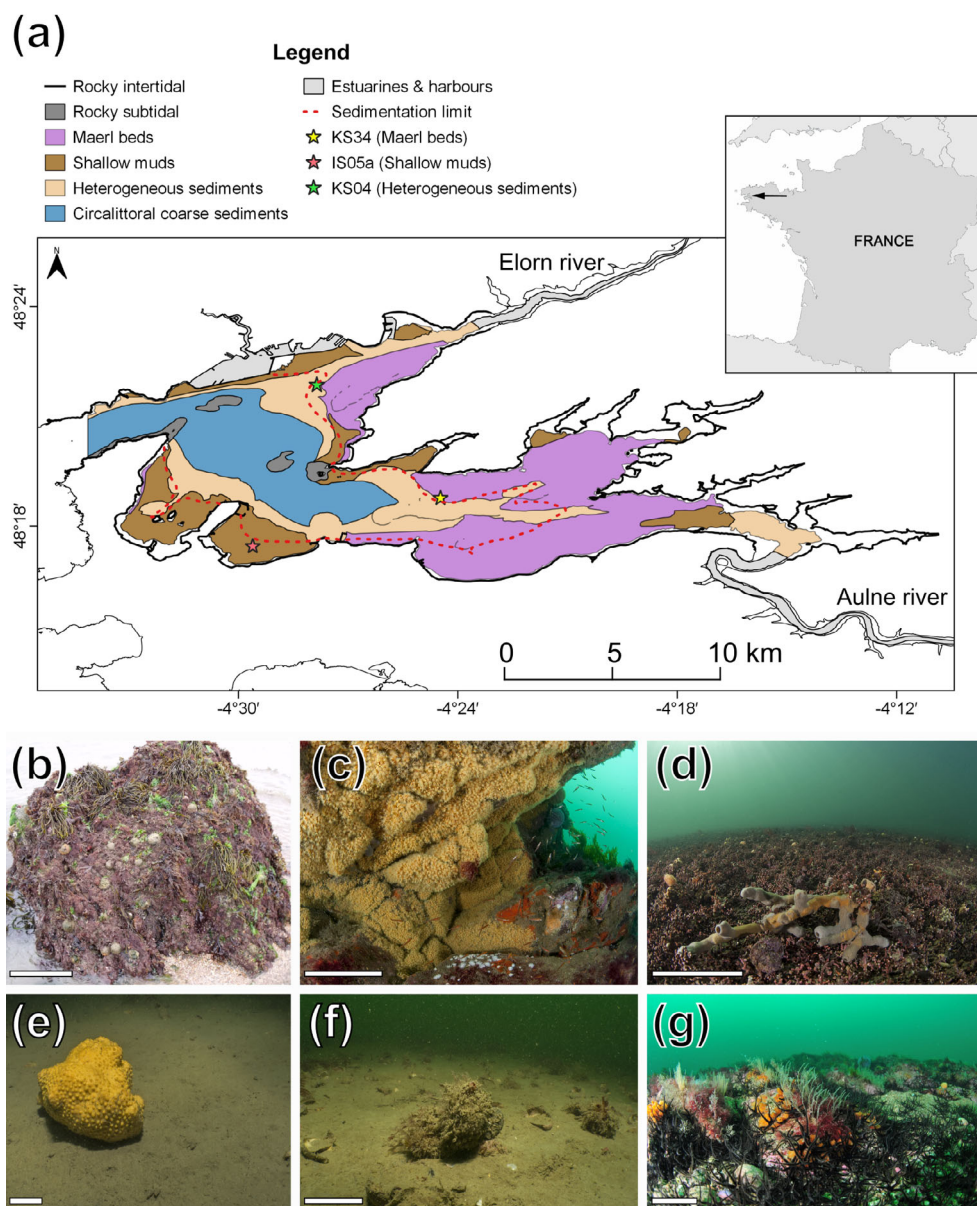


Fig. 1. (a) Map of the Bay of Brest (France), showing the six major habitats defined for this study according to their depth, substrate type, and sponge fauna. Estuaries and harbours, depicted in gray in the map, have not been considered in the study. The red dashed line indicates the limit of sedimentation in the Bay, under which the sedimentation rate is negligible. Stars indicate the geographical location of the examined cores. (b–g) General view of the habitats of the Bay: (b) rocky intertidal, (c) rocky subtidal, (d) maerl beds, (e) shallow muds, (f) heterogeneous sediments, and (g) circalittoral coarse sediments. Scale bars indicate 10 cm.

heterogeneous sediment and circalittoral coarse sediment located below 20 m depth were sampled using an epibenthic trawl over small transects (1 m wide \times 5–10 m long, trawl length precision = \pm 1 m; n = 28). Each sponge found within the quadrats or in the trawls was counted, taxonomically identified to the species level, and measured for volume and silica content (i.e., biogenic Si). To determine the sponge volume, the body shape of each individual was approximated to one or a sum of several geometric figures (e.g., sphere, cylinder, cone, rectangular plate, etc.) and the linear parameters needed to

calculate the volume (length, width, and/or diameter) were measured in situ using rulers (Maldonado et al. 2010). Counts and volume values in each habitat were normalized to m^2 . Nonsiliceous sponge species were taxonomically identified but not considered in the calculations.

Data distribution exploration of siliceous sponge abundance (i.e., number of individuals) and biomass (i.e., volume) per m^2 for each habitat and for the entire Bay showed that most datasets were not normally distributed (Shapiro–Wilk test) but slightly to moderate skew-positive distributed.

Table 1. Features of the benthic habitats of the Bay of Brest (France), including bottom area (10^6 m²), relative contribution (%), sampled area (m²), mean (\pm SD) depth (m), and richness of siliceous species of each habitat and the total Bay.

Habitat	Bottom area (10^6 m ²)	Sampled area (m ²)	Depth (m)	Siliceous species richness
RI	1.98 (1.5%)	23	0.0 (\pm 0.0)	4
RS	2.64 (2.0%)	31	12.4 (\pm 4.0)	31
MB	45.84 (34.4%)	40	5.4 (\pm 1.6)	19
SM	22.19 (16.7%)	17	5.1 (\pm 3.0)	2
HS	31.79 (23.9%)	36	11.4 (\pm 3.7)	16
CS	28.69 (21.6%)	23	25.6 (\pm 4.5)	32
Total	133.13 (100%)	170	9.9 (\pm 8.1)	45

CS, circalittoral coarse sediments; HS, heterogeneous sediments; MB, maerl beds; RI, rocky intertidal; RS, rocky subtidal; SM, shallow muds.

Consequently, nonparametric rank-based statistical analyses were performed and median and mean values were indicated in the Results. Statistical analyses were conducted using Sigmaplot version 14.5, from Systat Software Inc, with a significance level (p -value) of 5%.

The relationship between the mean siliceous sponge abundance (i.e., number of individuals per m²) and biomass (i.e., volume per m²) in each habitat was analyzed by Spearman rank correlation. Between-habitat differences in the sponge abundance and biomass per m² were examined by Kruskal–Wallis analysis and post hoc pairwise multiple comparisons between groups were conducted using the non-parametric Dunn's test.

To estimate sponge silica content in a given sponge volume, a plastic cylinder of known volume was filled with sponge tissue ($n = 3$ – 5 for each species, depending on availability), applying minimum compression. Sponge tissue samples were then dried at 60°C to constant dry weight (g), and desilicified by immersion in 5% hydrofluoric acid solution for 5 h, rinsed in distilled water three times for 5 min, and dried again at 60°C to constant dry weight (Maldonado et al. 2010). Silica content per unit of sponge volume (mg SiO₂ mL⁻¹ sponge) was calculated as the difference in weight before and after desilicification and multiplied by a factor of 0.8. Such a factor was applied to remove overestimates of the skeletal biogenic silica due to tiny sand grains (lithogenic silica) that might be embedded into the sponge tissues (Maldonado et al. 2010).

Mean skeletal content (mg SiO₂ mL⁻¹ sponge) of each species was subsequently used to estimate Si standing stock in the sponge communities per unit of bottom area in the six habitats of the Bay, and that at the ecosystem level. Between-habitat differences in mean sponge Si standing stock per m² were examined by a Kruskal–Wallis analysis, followed by pairwise Dunn's tests to identify significant differences between

groups. Finally, the relationship between skeletal content and sponge abundance per m² and that between skeletal content and sponge biomass per m² in the sponge communities of the Bay were also examined using regression analysis.

Dissolved silicon consumption by sponge communities

The annual consumption of dissolved Si (and consequently biogenic silica production) by the sponge communities of the Bay was estimated by using the Si consumption kinetic models developed elsewhere (López-Acosta et al. 2016, 2018) for the four dominant sponge species at the Bay (*Haliclona simulans*, *Hymeniacidon perlevis*, *Tethya citrina*, and *Suberites ficus*). The four species-specific kinetic models followed saturable Michaelis–Menten kinetics, as other demosponges investigated (Reincke and Barthel 1997; Maldonado et al. 2011). By knowing the monthly average dissolved Si availability in the bottom waters of the Bay over the last decade (2012–2021; Supporting Information Table S1) and the consumption kinetics of each of the four dominant species at the Bay, the average (\pm SD) annual dissolved Si consumption rate by these species was estimated. This average was then extrapolated to the rest of the sponge species in the Bay to estimate dissolved Si consumption by habitat and for the entire Bay, according to the estimated species sponge biomass per habitat (mL sponge m⁻²) and habitat bottom area (m²).

Sponge biogenic silica in surface sediments

The amount of sponge Si in the sediments was determined by analyzing surface sediment samples (defined herein as the upper-centimeter layer of sediment) from three stations from the shallow plateaus of the Bay of Brest (Fig. 1a). In the Bay, there are two major depositional environments with contrasting features: (1) the shallow terraces or plateaus, up to 10 m depth, where the fine sediment that regularly arrives through the rivers' discharges is homogeneously deposited, and (2) the deepest bottoms, up to 40 m depth, where the strong tidal currents prevent the fine sediment from being deposited on the bottom (Salomon and Breton 1991; Gregoire et al. 2017; Lambert et al. 2017). The latter are located mainly in the central zone of the Bay and the two paleo-channels that cross each of the basins of the Bay from the rivers' mouths to the central zone, where they converge (see Fig. 1 in Gregoire et al. 2017). This depositional configuration was originated by the action of successive sea-level low stands and it has been preserved over the last millennia by the effect of tidal currents in deep-water areas, which keep the inherited shape by preventing the deposition of the fine sediment supplied by rivers (Gregoire et al. 2016, 2017). As a consequence of this hydrodynamic regime, the fine sediment does not settle on the deepest areas of the Bay, the sediments of which mainly consist of coarse particles such as gross fragments of shells and small pebbles (Gregoire et al. 2016). On the contrary, the fine sediment settles all over the shallow plateaus, which are less affected by the tidal currents. Hence, the shallow plateaus

account for virtually the total area of sediment deposition in the Bay bottoms (Ehrhold et al. 2016). These shallow plateaus, which account for about half of the Bay surface, are mainly covered by maerl beds, shallow muds and partially by heterogeneous sediments (Fig. 1a; Table 2).

To estimate the amount of sponge silica in the surface sediments of the Bay, one core was sampled at each benthic habitat represented at the shallow plateaus: core SRQ3-KS34 from maerl beds, core SRQ1-IS05 from shallow muds, and core SRQ3-KS04 from heterogeneous sediments (Fig. 1a; Table 2). Present-day sedimentation rates were estimated from radiocarbon dating of surface sediment in the cores (Gregoire et al. 2017; Ehrhold et al. 2021). The bottoms of the deepest areas of the Bay, on which sedimentation rates are negligible (Ehrhold et al. 2016), were interpreted as null contributors to the sponge silica accumulation in the Bay (see below).

To quantify the sponge silica in the surface sediment layer, one to three sediment subsamples of 10 mg each were collected from the upper 1-cm layer of each core and subsequently processed by light microscopy, following the methodology described in Maldonado et al. (2019). Briefly, sediment subsamples were transferred to test tubes, boiled in 37% hydrochloric acid to remove calcareous materials, then in 69% nitric acid to complete digestion of organic matter, rinsed in distilled water, and sonicated for 15 min to minimize sediment aggregates. The sediment suspension was then pipetted out and dropped on a microscope glass slide to measure the volume of each skeletal piece (spicules). A total of 48,320 spicules, either entire or fragmented, were examined in 230 slides with phase contrast microscopes. Using digital cameras and morphometric software (ToupView, ToupTek Photonics), the volume of each spicule or spicule's fragment was estimated by approximating its shape to one or the sum of several geometric figures (Maldonado et al. 2019). Measured volumes of sponge silica were subsequently converted into Si mass, using the average density of 2.12 g mL^{-1} for sponge silica (Sandford 2003).

To determine the reservoir of sponge silica in the surface sediment of the Bay, the obtained mass of sponge silica per gram of sediment in each core was extrapolated to the area of

each benthic habitat over the sedimentation limit (Ehrhold et al. 2016), delimited with a red dashed line in Fig. 1. It means that the sponge silica mass per gram of sediment from core SRQ3-KS34 was extrapolated to 40.06 km^2 , that of core SRQ1-IS05 to 17.21 km^2 , and that of core SRQ3-KS04 to 9.18 km^2 (Table 2). By combining these parameters and the wet-bulk density of the surface sediment of each core (Table 2), the amount of sponge Si reservoir in surface sediments was calculated. Sponge Si deposition rate was estimated from the amount of sponge Si determined in the surface sediments of each core location and the sedimentation rate (Table 2). Sponge Si burial rate, that is, the amount of sponge silica that is ultimately preserved in the sediments, was estimated from the rate of sponge Si deposited annually in the surface sediments and the average percentage estimated for sponge Si preservation in sediments of marine continental shelves (i.e., $52.7\% \pm 29.8\%$; Maldonado et al. 2019). The contribution of sponges to the Si benthic efflux from the sediments of the Bay was calculated as the difference between the sponge Si deposition and burial rates.

Sponge silica budget in a coastal ecosystem: The Bay of Brest

The quantified stocks and fluxes of sponge Si were used to build a sponge Si budget for the Bay of Brest. These results were discussed in the context of previous studies and compared with those reported in the literature for the community of planktonic diatoms in the Bay.

Results

General features of the sponge assemblages

The survey of the sponge fauna at the Bay of Brest revealed a total of 53 sponge species, most of them belonging to the class Demospongiae ($n = 51$), and only 2 species belonging to the class Calcarea (Supporting Information Table S2). Species from classes Hexactinellida and Homoscleromorpha were not found. Forty-five (85%) of the 53 identified species had siliceous skeletons (Table 1). The other eight were nonsiliceous sponge species with a skeleton made of either calcium

Table 2. Summary of core features including core label, coordinates, depth (m), average (\pm SD) sedimentation rate (cm yr^{-1}), wet-bulk density ($\text{g sed. cm}^{-3} \text{ sed.}$), the benthic habitat compartment they represent, and the extension of the benthic habitat over the sedimentation limit of the Bay (km^2). Present-day sedimentation rates for the surface sediments of each core were estimated from ^{14}C radiocarbon dating in Gregoire et al. (2017) and Ehrhold et al. (2021).

Core label	Coordinates		Depth (m)	Sedimentation rate (cm yr^{-1})	Wet-bulk density (g cm^{-3})	Benthic habitat compartment	Compartment extension (km^{-2})
	Latitude	Longitude					
SRQ3-KS34	48°18.760'N	4°24.474'W	10	0.037 (\pm 0.003)	1.684	Maerl beds (MB)	40.06
SRQ1-IS05a	48°17.441'N	4°29.609'W	7	0.090 (\pm 0.002)	1.660	Shallow muds (SM)	17.21
SRQ3-KS04	48°21.858'N	4°27.857'W	7	0.077 (\pm 0.001)	1.660	Heterogeneous sediments (HS)	9.18

carbonate ($n = 2$) or skeletal protein ($n = 6$). Nonsiliceous sponges were not considered in the following quantifications of sponge abundance and biomass.

Sampling yielded a total of 1807 sponge individuals for which volume was determined (Table 1). At the Bay level, the siliceous sponge fauna averaged (mean \pm SD) 10.6 ± 11.1 individuals m^{-2} and a biomass of 0.24 ± 0.35 liters of living sponge tissue m^{-2} . The large variation associated (i.e., SD) to the sponge abundance and biomass normalized per m^2 is derived from the patchy spatial distribution of the sponges at both intra- and inter-habitat level (Fig. 2). In contrast, the standard error (SE) of the mean ($= SD/\sqrt{N}$) is low (SE of sponge abundance = 0.85; SE of sponge biomass = 0.03), indicating that mean values are accurate. Spearman's correlation involving the six habitats revealed a strong positive correlation between the mean abundance and the biomass of siliceous sponges per m^2 of sampled bottom ($N = 6$, $\rho = 0.886$, $p = 0.033$). This relationship informs that body size is more or less uniformly distributed across species and specimens of the different habitats.

At the habitat level, there were large between-habitat differences in both sponge abundance and biomass (Fig. 3). The total number of siliceous sponges per m^2 significantly differs between habitats ($H = 89.059$, $df = 5$, $p < 0.001$). Highest sponge abundance per m^2 were reported in the maerl beds and rocky subtidal habitats, averaging 24.6 ± 26.2 and 16.4 ± 9.3 individuals m^{-2} , respectively (Fig. 2). The median siliceous sponge abundance per m^2 in the benthic communities of the maerl beds and rocky subtidal habitats (13 and 16 individuals m^{-2} , respectively) were significantly higher than that in the other habitats (Fig. 3a). Biomass of siliceous sponges ($L m^{-2}$) also differed significantly between habitats ($H = 78.324$, $df = 5$, $p < 0.001$). A posteriori pairwise comparison revealed that median sponge biomass per m^2 at the rocky subtidal habitat ($0.4 L m^{-2}$), which showed the highest mean sponge biomass per sampled bottom ($3.8 \pm 9.7 L m^{-2}$), was significantly higher than that at the heterogeneous sediments ($0.05 L m^{-2}$; mean \pm SD: $0.16 \pm 0.38 L m^{-2}$) and the rocky intertidal ($0.07 L m^{-2}$; mean \pm SD: $0.12 \pm 0.13 L m^{-2}$) habitats. Median sponge biomass per m^2 at maerl beds ($0.14 L m^{-2}$; mean \pm SD: $0.31 \pm 0.32 L m^{-2}$), which ranked second, did not differ significantly from that at the rocky subtidal, either at the heterogeneous sediments and rocky intertidal habitat. Median sponge biomass per m^2 at shallow muds and circalittoral coarse sediments were similar to each other and significantly lower than those at the rest of habitats in the Bay (Fig. 3b,c).

Silicon standing stock in the sponge communities

The importance of the siliceous skeleton content per mass unit of sponge tissue varied largely between sponge species (Table 3). It ranged from 29.8 ± 2.9 to 145.6 ± 14.2 mg SiO_2 per mL of living sponge tissue (Table 3), accounting for 19.6% to 63.5% of the specific dry weight (DW). The average skeletal

content estimated for the siliceous sponge fauna of the Bay of Brest was 59.6 ± 27.1 mg $SiO_2 mL^{-1}$ ($45.8 \pm 10.6\%$ SiO_2/DW). From these figures, it is estimated that the Si standing stock in the sponge fauna of the Bay of Brest is 9.1 ± 14.1 g Si m^{-2} . Nevertheless, there are large between-habitat differences in the sponge Si standing stock per m^2 (Fig. 3b,c). The highest mean Si standing stock occurred in the rocky subtidal habitat (151.1 ± 387.6 g Si m^{-2}). At this habitat, large specimens of *Cliona celata* were common (mean abundance = 0.5 ± 0.7 individual m^{-2} , mean biomass = 7.4 ± 13.5 L individual $^{-1}$). The large specimens of this species, which is moderately silicified (85.6 ± 7.2 mg $SiO_2 mL^{-1}$; Table 3), are responsible for the 89.2% of the total biomass and Si standing stock of the rocky subtidal habitat. The maerl beds ranked second in Si standing stock, with an average of 10.0 ± 10.7 g Si m^{-2} (Fig. 3b,c). In this habitat there is large abundance of sponges (24.6 ± 26.2 individuals m^{-2}) with body size ranging from small to medium (mean biomass = 12.4 ± 37.1 mL individual $^{-1}$). Four of the 19 siliceous sponge species identified at this habitat accounted for 84% of the total sponge Si standing stock (*H. simulans*, *H. perlevis*, *T. citrina*, and *S. ficus*). A Kruskal–Wallis analysis confirmed that the between-habitat differences in sponge Si standing stock per m^2 are statistically significant ($H = 71.701$, $df = 5$, $p < 0.001$). The pairwise comparison of mean Si standing stock revealed the same pattern of between-habitat differences than that obtained in the pairwise comparison of mean sponge biomass (Fig. 3b,c). Further analysis indicated a significant linear relationship ($n = 170$, $R^2 = 0.999$, $p < 0.0001$) between sponge biomass and Si standing stock per m^2 across habitats (Fig. 4).

By integrating the average Si content of the sponges across the bottom area of each habitat, a total Si standing stock of $1215 \pm 1876 \times 10^3$ kg Si ($43.3 \pm 66.8 \times 10^6$ mol Si) in the sponge communities of the Bay of Brest was estimated. The small-scale patchiness in the spatial distribution of the sponges within a habitat causes some sampling quadrats to contain many sponges while others contain very few or none. This effect, when propagated for the calculation of the global mean of the Bay, results in a large SD value. In addition, about 90% of the stock is accumulated in the sponge fauna of three habitats, which—in order of contribution—are the maerl beds, the rocky subtidal, and the heterogeneous sediments.

Dissolved silicon consumption by sponge communities

The average monthly concentrations of dissolved Si at the bottom waters of the Bay ranged from 2 to 13 μM (Supporting Information Table S1). Applying these concentrations to the silicon consumption kinetic models previously obtained for the dominant species in the Bay (López-Acosta et al. 2016, 2018), the most abundant species at the Bay (*H. perlevis*, 68.6 ± 85.1 mL m^{-2}) consumed 7.2 ± 8.9 mmol Si $m^{-2} yr^{-1}$. Interestingly, the species *T. citrina* and *S. ficus*, which show comparatively lower biomass records in the Bay (24.5 ± 34.1 and 7.7 ± 13.3 mL m^{-2} , respectively), had similar rates of Si

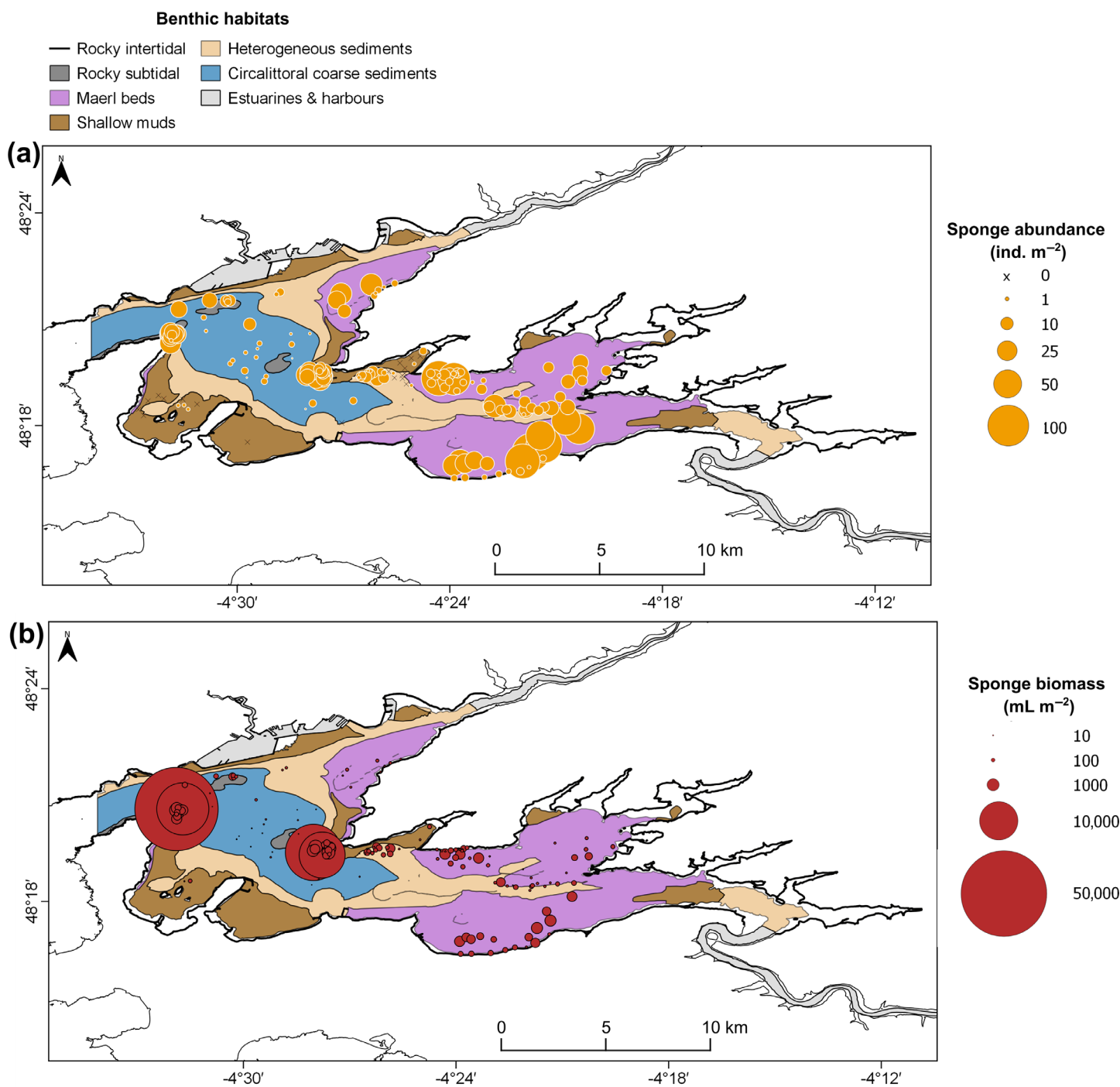


Fig. 2. Map of the Bay of Brest (France), showing the spatial distribution of (a) sponge abundance and (b) biomass per square meter. Estuaries and harbors, depicted in gray in the map, have not been considered in the study.

consumption (7.5 ± 10.5 and 7.1 ± 21.0 mmol Si m⁻² yr⁻¹, respectively). This is because their affinity for Si is higher (affinity coefficient, $V_{\max}/K_M = 6.9 \times 10^{-3}$ and 4.4×10^{-3} $\mu\text{mol Si h}^{-1}$ sponge-mL⁻¹ Si- μM^{-1} for *T. citrina* and *S. ficus*, respectively, compared to 2.1×10^{-3} $\mu\text{mol Si h}^{-1}$ sponge-mL⁻¹ Si- μM^{-1} for *H. perlevis*).

Not surprisingly, most of the sponge Si consumption of the Bay occur in the rocky subtidal habitat and maerl beds, where sponges are very abundant and they show moderate to large biomass records (Figs. 2, 3). The rocky subtidal habitat, which represents only 2.0% of the Bay bottom but hosts about 30% of the total sponge biomass in the Bay, shows an annual

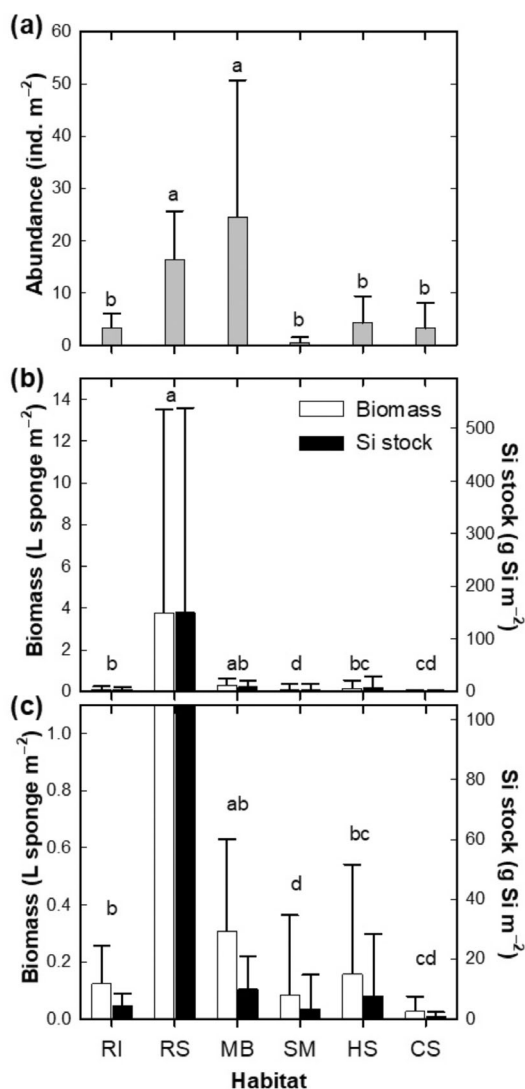


Fig. 3. Summary of (a) average (\pm SD) abundance (individuals m^{-2}), (b) biomass (L sponge m^{-2} ; white bars), and silicon (Si) standing stock (g Si m^{-2} ; black bars) in the siliceous sponge fauna of the habitats of the Bay of Brest (France). Significant between-habitat differences of (a) abundance and (b) biomass and Si stock of the sponge fauna are indicated with different letters according to the results of Kruskal–Wallis analysis and the a posteriori pairwise Dunn's tests. (c) This graph makes visible the contribution of the habitats with sponge biomass and Si standing stock records lower than 1 L sponge m^{-2} and 100 g Si m^{-2} . RI, rocky intertidal; RS, rocky subtidal, MB for maerl beds, SM for shallow muds, HS for heterogeneous sediments, and CS for circalittoral coarse sediments.

sponge Si consumption rate of $74.2 \pm 141.4 \times 10^3$ kg Si yr^{-1} ($2.6 \pm 5.0 \times 10^6$ mol Si yr^{-1}). The maerl beds, in which *H. perlevis*, *T. citrina*, and *S. ficus* are abundant in both terms of number of individuals and biomass, shows an annual Si consumption rate of $73.6 \pm 112.7 \times 10^3$ kg Si yr^{-1} ($2.6 \pm 4.0 \times 10^6$ mol Si yr^{-1}). Collectively, the assemblage of siliceous sponges in the Bay is estimated to consume annually $200.8 \pm 372.1 \times 10^3$ kg Si yr^{-1} ($7.2 \pm 13.2 \times 10^6$ mol Si yr^{-1}).

Sponge biogenic Si in sediments

The surface sediments (i.e., the upper 1-cm layer) of cores SRQ3-KS34, SRQ1-IS05a, and SRQ3-KS04, contained, respectively, a total of $1.07 (\pm 0.05)$, 1.30 , and 0.32 million spicules or spicule fragments per g of sediment, with an average spicule content of $0.89 (\pm 0.51)$ million spicules g^{-1} sediment for the set of studied cores (Table 4). In all cores, most spicules (98.3–99.1%) were recognized as megascleres, either entire or fragmented. The microscopic study of the surface sediment in the cores showed only small between-area differences in the mass of sponge biogenic Si, which ranged from 0.799 to 2.505 mg Si g^{-1} sediment (Table 4). The average content of sponge biogenic Si in the sediments of the Bay of Brest was $1.565 (\pm 0.866)$ mg Si g^{-1} sediment.

Sponge Si deposition rates in the studied areas ranged from 9.4 to 64.4×10^3 kg Si yr^{-1} , depending on the habitat (Table 5). When deposition rates were extrapolated to the total extension of the shallow plateaus (i.e., 66.45 km²), it resulted in a mean deposition rate of $108.7 \pm 9.1 \times 10^3$ kg Si yr^{-1} ($3.9 \pm 0.3 \times 10^6$ mol Si yr^{-1}). The sponge Si burial rate was then calculated from the deposition rate and the average preservation rate of sponge silica determined by Maldonado et al. (2019) for continental-shelf sediments. This approach yielded an average burial rate of sponge silica in the sediments of the shallow plateaus of $57.3 \pm 18.2 \times 10^3$ kg Si yr^{-1} ($2.0 \pm 0.6 \times 10^6$ mol Si yr^{-1}). The differences between deposition and burial rate is, in the long run, the sponge contribution to the benthic Si efflux from sediments, which was estimated to be $51.4 \pm 17.7 \times 10^3$ kg Si yr^{-1} ($1.8 \pm 0.6 \times 10^6$ mol Si yr^{-1}) for the shallow plateaus of the Bay (Table 5).

According to the depositional environments of the Bay, the deep sediments were not considered in the calculations of the total sponge Si reservoir and sediment fluxes rates (see Methods). This is also supported by the sponge spatial distribution at the Bay, which shows that in the deepest areas sponges are particularly low abundant (3.2 ± 4.9 ind. m^{-2}) and their contribution to the Si standing stock is significantly low (0.8 ± 1.4 g Si m^{-2} ; Fig. 3). By extrapolating the sponge silica content determined in the surface sediments of the Bay (Table 5), a total sponge silica reservoir in the surface sediment layer of the Bay of Brest of $1775 \pm 162 \times 10^3$ kg Si ($63.2 \pm 5.8 \times 10^6$ mol Si) was estimated.

Discussion

Sponge fauna within the Bay of Brest

The survey of sponge fauna in the Bay of Brest revealed that sponges are widely present in most of the habitats (17–36 spp. per habitat; Table 1; Fig. 2; Supporting Information Table S2). Only two habitats, the shallow muds and the rocky intertidal, showed low sponge species richness (≤ 4 species per habitat; Table 1; Supporting Information Table S2). These two habitats, the former characterized by muddy bottoms and scanty hard substratum and the latter by periodic air

Table 3. Summary of biogenic silica (i.e., SiO₂) standing stock in the sponge assemblages of the Bay of Brest (France). Average (\pm SD) silica content per unit of volume of living sponge tissue (mg SiO₂ mL⁻¹) of each siliceous sponge species and average (\pm SD) sponge Si stock per square meter (mg Si m⁻²) in each habitat and for the total ecosystem of the Bay of Brest.

Sponge species	Sponge contribution to the Si standing stock (mg Si m ⁻²)														
	Biogenic Si content (mg SiO ₂ mL ⁻¹)			RI		RS		MB		SM		HS		CS	
	Mean	SD		Mean	SD	Mean	SD	Mean	SD	Mean	SD	Mean	SD	Mean	SD
<i>Amphilectus fucorum</i>	36.13	4.79		222.88	655.79	27.59	124.16					3.17	13.25	5.31	25.44
<i>Antho inconstans</i>	33.27	4.25		101.84	567.05										
<i>Biernia variantia</i>	45.38	4.86		4.79	26.67										
<i>Bubaris vermiculata</i>	96.21	11.21												6.77	24.33
<i>Chalinula cf. limbata</i>	43.92	6.96		31.79	177.00										
<i>Ciocalypta penicillus</i>	103.61	0.39		374.14	1456.86							0.77	4.64	0.76	2.39
<i>Clathria strepsitoxa</i>	29.78	2.89		194.81	519.89							1.11	6.67	64.09	134.54
<i>Clypea celata</i>	85.58	7.24		134,576.89	389,757.49					2961.26	11,145.37			102.10	122.41
<i>Clypea lobata</i>	78.15	5.94												0.28	0.96
<i>Halichondria bowerbanki</i>	58.33	1.83		7.92	32.41	116.13	724.07							3.97	14.96
<i>Halichondria panicea</i>	55.40	11.30	134.18	60.07	197.04	268.83	677.52								
<i>Halichondria sp.</i>	71.38	0.77		434.84	949.91	73.18	336.72								
<i>Haliclona angulata</i>	39.55	6.92		17.10	95.19	6.91	18.02								
<i>Haliclona cinerea</i>	37.79	4.50												25.17	69.19
<i>Haliclona fibulata</i>	53.64	6.23												1.48	3.37
<i>Haliclona fistulosa</i>	52.52	21.55		24.29	135.26	18.65	116.43							132.65	386.64
<i>Haliclona rosea</i>	32.94	5.41		13.16	45.12	116.88	253.13							11.64	55.80
<i>Haliclona simulans</i>	74.95	16.47		554.65	1613.25	613.86	1374.11					20.32	115.42	1.97	6.53
<i>Hemimycale columella</i>	49.41	7.03		621.31	1625.25	37.82	165.58					152.11	411.44	57.56	150.02
<i>Hymedesmia cf. occulta</i>	35.99	6.52										8.66	51.97	1.10	5.27
<i>Hymedesmia coriacea</i>	32.58	6.30		0.49	2.74	5.81	27.81							0.88	3.20
<i>Hymedesmia jecusculum</i>	36.29	5.67		21.73	86.53									0.65	3.11
<i>Hymedesmia lenta</i>	30.47	5.05		7.75	43.17										
<i>Hymeniacidon perlevis</i>	48.88	6.18	1975.23	794.85	1854.75	3968.75	5403.69								
<i>Iophon hyndmani</i>	42.56	3.16													
<i>Iophon nigricans</i>	43.77	2.11													
<i>Mycale contarenii</i>	62.69	7.71		86.50	222.88	20.88	91.83							7.48	27.56
<i>Mycale macilenta</i>	52.87	5.32		795.91	2050.78	0.14	0.88							54.60	248.94
<i>Myxilla fimbriata</i>	50.77	4.34		128.62	340.78									5.36	16.97
<i>Myxilla rosacea</i>	42.64	4.02												200.99	905.76
<i>Pachymatisma johnstonia</i>	116.70	22.01		3918.18	15,445.96										
<i>Paratimea constellata</i>	66.94	4.07													
<i>Phorbas ficitus</i>	93.20	5.22		420.82	2061.94	497.65	1419.77								
<i>Phorbas plumosus</i>	40.95	15.92		122.27	649.18	52.54	160.68								
<i>Polymastia boletiformis</i>	58.91	11.51		58.63	326.44										
<i>Polymastia penicillus</i>	71.41	7.84	1.27	230.17	1258.52									0.29	1.38
<i>Protosuberites cf. denhartogi</i>	57.84	4.85		77.23	287.25									0.10	0.46
<i>Raspailia ramosa</i>	56.76	5.60													
<i>Spanioplon armaturum</i>	32.48	3.26		463.15	920.96									1.69	8.12
<i>Stelligera stuposa</i>	44.70	3.04		76.69	238.29									0.24	0.96
<i>Suberites ficus</i>	114.77	12.45												0.74	3.48
<i>Suberites massa</i>	96.02	4.70				995.23	6105.84			582.80	1801.65				
<i>Tedania anhelans</i>	34.90	6.42		0.25	1.60	105.64	493.25								
<i>Tethya citrina</i>	145.57	14.17	2166.28	3780.43	15,889.11	3103.96	5192.50							122.48	266.90
<i>Timea crassa</i>	93.89	4.14												76.76	150.91
Total	59.61	27.07	4283.08	4191.32	151,079.97	387,576.21	10,035.84	10,742.40	3544.06	11,126.45	7737.09	20,560.60		161.92	608.25

CS, circalittoral coarse sediments; HS, heterogeneous sediments; MB, maerl beds; RI, rocky intertidal; RS, rocky subtidal; SM, shallow muds.

exposures during low tides, hosted only a handful of species able to deal with those harsh conditions (Supporting Information Table S2).

The taxonomic composition and spatial distribution of the sponge fauna significantly differed between habitats (Table 1; Fig. 2). Spatial heterogeneity has been widely reported for

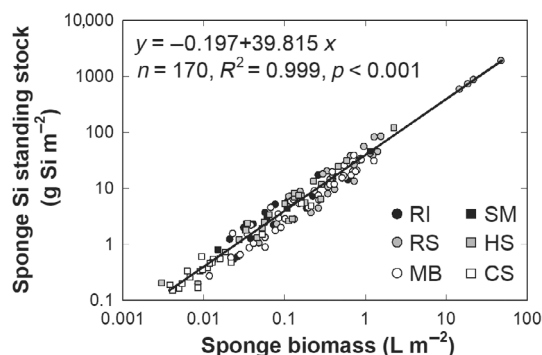


Fig. 4. Relationship between silicon (Si) standing stock (g Si m^{-2}) and biomass (L m^{-2}) of siliceous sponges per m^2 of sampled bottom at the Bay of Brest (France). Symbols represent the location of the data (i.e., habitat; abbreviations mean: RI, rocky intertidal; RS, rocky subtidal; MB, maerl beds; SM, shallow muds; HS, heterogeneous sediments; CS, circalittoral coarse sediments). Sponge Si stock and biomass are shown in logarithmic scale.

Table 4. Summary of the results obtained during the microscopic examination of the surface sediments of the Bay of Brest. Average (\pm SD, when available) spicule counts (in millions per gram of sediment), contribution (%) of megascleres (spicules longer than $100 \mu\text{m}$) and microscleres (spicules shorter than $100 \mu\text{m}$), and mass of sponge silica per gram of sediment for each core are indicated, as well as for the set of study cores.

Core label	Benthic habitat	No. of spicules ($N \times 10^6 \text{ g}^{-1} \text{ sed.}$)	Spicule-type contribution (%)		Sponge Si in surface sed. ($\text{mg Si g}^{-1} \text{ sed.}$)
			Megascleres	Microscleres	
SRQ3-KS34	Maerl beds (MB)	1.07 (± 0.05)	99.1 (± 0.3)	0.9 (± 0.3)	1.391 (± 0.241)
SRQ1-IS05a	Shallow muds (SM)	1.30	99.0	1.0	2.505
SRQ3-KS04	Heterogeneous sediments (HS)	0.32	98.3	1.7	0.799
Average (\pm SD)		0.89 (± 0.51)	98.8 (± 0.4)	1.2 (± 0.4)	1.565 (± 0.866)

Table 5. Sponge silicon (Si) stock in the surface sediments of each depositional environment of the Bay of Brest, along with the deposition, burial and benthic flux rate of sponge Si. Area (km^2) to which the sponge Si in sediments was extrapolated is indicated. These areas do not correspond to the total habitat extension but to the habitat area that is above the sedimentation limit of the Bay (indicated with a red dashed line in Fig. 1a) for cores representing the shallow depositional plateaus.

Core label	Benthic habitat	Area (km^2)	Sponge Si stock Reservoir (10^3 kg Si)	Sponge Si fluxes		
				Deposition rate ($10^3 \text{ kg Si yr}^{-1}$)	Burial rate ($10^3 \text{ kg Si yr}^{-1}$)	Benthic flux ($10^3 \text{ kg Si yr}^{-1}$)
SRQ3-KS34	Maerl beds (MB)	40.06	937.93	34.91	18.39	16.52
SRQ1-IS05a	Shallow muds (SM)	17.21	715.41	64.39	33.92	30.47
SRQ3-KS04	Heterogeneous sediments (HS)	9.18	121.70	9.38	4.94	4.44
Total		66.45	1775.04	108.68	57.25	51.43

sponge distributions across all oceans, with a variety of biological and physical reasons behind it (Hooper 2019). Among the habitats of the Bay, the rocky subtidal is the one with the highest sponge biomass per unit area ($3.8 \pm 9.7 \text{ L m}^{-2}$; Fig. 3b), reaching values similar to those reported in some emblematic sponge aggregations in tropical and polar latitudes (Maldonado et al. 2017 and references therein). The maerl beds, which accounted for about one third of the total surface of the Bay (Table 1), hosted most of the sponge individuals and biomass of the Bay—79% \pm 46% of the total number of sponges (1416 ± 1474 million of individuals) and about 44% \pm 23% of the total sponge volume ($31.9 \pm 47.0 \times 10^6 \text{ L}$) estimated at the Bay of Brest. Thus, the maerl beds of the Bay serve as substrate to highly diverse and abundant sponge fauna, which along with other benthic organisms, make these bottoms real sponge and biodiversity hotspots, similar to what has been reported for maerl beds from other ocean regions (Sciberras et al. 2009; Ávila and Riosmena-Rodríguez 2011; Neill et al. 2015).

Biogenic silica stock as sponge skeletons

Our results indicate that a substantial amount of the biogenic silica stock of the Bay of Brest is in the form of sponge silica, in both the living sponge fauna and the sediments of

the Bay (Fig. 5). In the benthic communities, the Si standing stock in the form of sponge skeletons totaled $1215 \pm 1876 \times 10^3$ kg of Si, that is, 45 times larger than that of the planktonic diatoms living in the water column (see below and Fig. 5). The siliceous skeleton within the sponges accounted for 19.6–63.5% of the sponge dry weight, depending on the species (average value = $45.8\% \pm 10.6\%$ $\text{SiO}_2/\text{DW} = 59.6 \pm 27.1$ $\text{mg SiO}_2 \text{ mL}^{-1}$; Table 3). Similar biogenic Si content and between-species variability was also reported in a sponge-rich community of the Belizean Mesoamerican Barrier Reef (53.4 ± 6.1 $\text{mg SiO}_2 \text{ mL}^{-1}$; Maldonado et al. 2010).

To date, only few studies have measured the amount of Si trapped in sponge communities of shallow-water ecosystems. The sponge Si standing stock per m^2 in the Bay of Brest (9.1 ± 14.1 g Si m^{-2}) is about four times higher than that found in the sublittoral population of the encrusting demosponge *Crambe crambe* at the Catalan coast of the NW Mediterranean (2.5 ± 2.7 g Si m^{-2} ; Maldonado et al. 2005) and, interestingly, similar to that measured in the sublittoral sponge-rich assemblages of the Belize section of the Mesoamerican Barrier Reef (12.0 g Si m^{-2} ; Maldonado et al. 2010). The sponge Si standing stock of the Bay of Brest is also similar to that found at bathyal depths at the westward slope of the Mauna Loa Volcano of Hawaii (12.6 g Si m^{-2} ; Maldonado

et al. 2005), where a dense monospecific population of the highly silicified hexactinellid *Sericolophus hawaiiicus* occurs. Higher records of Si sponge stocks have only been reported from (1) the monospecific sponge ground of the hexactinellid *Vazella pourtalessii* at the Nova Scotian continental shelf, Canada (43.8 ± 74.6 g Si m^{-2} ; Maldonado et al. 2021); (2) the continental margins of Antarctica (178 g Si m^{-2} ; Gutt et al. 2013), where heavily silicified demosponges and hexactinellids co-occur; and (3) the singular epibathyal reefs of the hexactinellid *Aphrocallistes vastus* in British Columbia (Canada), where high densities of heavily silicified individuals grow on exposed skeletons of dead sponges, leading to outstanding accumulations of sponge silica in the form of siliceous reefs (4238 ± 924 g Si m^{-2} ; Chu et al. 2011). Altogether, these results support the idea that living sponge communities are transient silicon sinks (Maldonado et al. 2005, 2010) and suggest that relevant standing stocks of sponge silica are likely to occur not only in deep-sea and polar latitudes but also in shallow-water ecosystems from temperate latitudes, in which diverse and abundant sponge populations may easily develop (Van Soest et al. 2012; Maldonado et al. 2017).

The amount of sponge silica accumulated in only the surface (upper centimeter) sediment layer of the Bay of Brest ($1775 \pm 162 \times 10^3$ kg Si) falls in the same order of magnitude than that accumulated in the living sponge fauna of the Bay

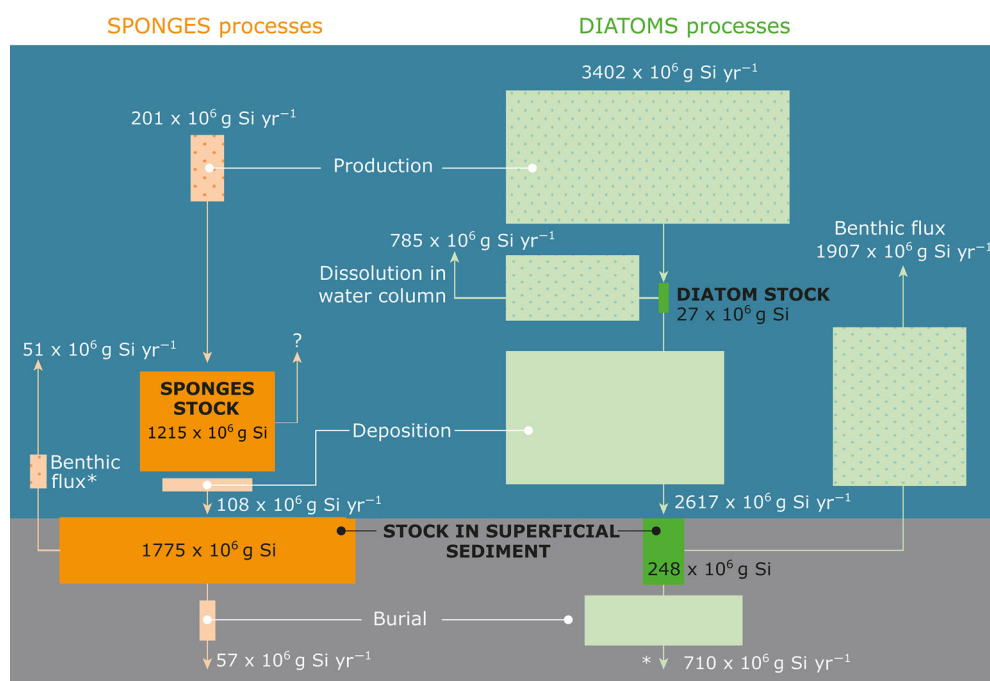


Fig. 5. Scheme summarizing the silicon stocks and fluxes through the sponge and planktonic diatom communities of the Bay of Brest (France). Stocks and fluxes of silicon (Si) mediated by sponges are in orange, and those mediated by diatoms are in green. Stocks of biogenic silica are indicated in tons of Si. Fluxes of silicic acid, with a dotted pattern, and those of biogenic silica, lacking the dotted pattern, are indicated in tons of Si per year. The size of the boxes representing both stocks and fluxes is proportional to their rate. Fluxes of Si through diatoms are from Ragueneau et al. (2005), stock of biogenic silica in planktonic diatoms has been calculated from Beucher et al. (2004), and reservoir of diatom silica in surface sediments are from Song and Ragueneau (2007). Asterisks refer to fluxes derived indirectly.

($1215 \pm 1876 \times 10^3$ kg; Fig. 5). The Si stock in the surface sediments is in the form of siliceous spicules that reach the sediments after sponge death (Chou et al. 2012; Lukowiak et al. 2013; Maldonado et al. 2019), the abundance of which appears to be proportional to the silica standing stock in the sponge communities living nearby (Bavestrello et al. 1996; Lukowiak et al. 2013). The amounts of sponge silica deposited in surface sediments of the Bay of Brest ($0.799\text{--}2.505$ mg Si g^{-1} sediment; Table 4) are among the highest determined in surface sediments of continental margins from different oceans and seas ($0.014\text{--}2.572$ mg Si g^{-1} sediment; Sañé et al. 2013; Maldonado et al. 2019). For instance, the amount of sponge silica determined in the surface sediments of the shallow muds (2.505 mg Si g^{-1} sediment, core SRQ1-IS05a; Table 4) is nearly identical to that determined in the surface sediments of the slope of the Bransfield Strait in Antarctica (2.572 ± 0.861 mg Si g^{-1} sediment; Maldonado et al. 2019), where dense sponge aggregations occur (Ríos and Cristobo 2014; Kersken et al. 2016; Gutt et al. 2019) and similar sedimentation rates have been reported ($0.057\text{--}0.117$ cm yr^{-1} ; Masqué et al. 2002). Combining the cores examined in this study (1.565 ± 0.241 mg Si g^{-1} sediment), the sediments of the Bay had about 60% more sponge silica than the average estimated for the sediments of continental margins in the global ocean (0.924 ± 0.854 mg Si g^{-1} sediment; Maldonado et al. 2019), indicating that sediments from areas where sponges abound become an important reservoir of biogenic silica.

Silicon cycling through the sponge assemblage

The siliceous skeletons produced by the sponges as part of their annual growth are progressively accumulated within the sponge body for the lifespan, which is thought to range from years to decades or centuries in shallow-water sponge species from temperate latitudes (McMurray et al. 2008; Teixidó et al. 2011; McGrath et al. 2018). When a sponge dies or part of its body is removed or damaged by either natural or anthropogenic processes, the siliceous spicules within the sponge tissue are freed and end deposited on the surface sediments (Chou et al. 2012; Lukowiak et al. 2013; Maldonado et al. 2019). In the Bay of Brest, the deposition of sponge silica was estimated to be $108 \pm 9 \times 10^3$ kg Si yr^{-1} (Fig. 5). Such average rate is about twice smaller than the average rate at which sponges produce silica in the Bay ($201 \pm 372 \times 10^3$ kg Si yr^{-1} ; Fig. 5). Note that the large variation associated (i.e., SD) to the sponge Si production is related to the patchy spatial distribution of the sponge biomass in the Bay, the records of which were used to determine the sponge Si standing stock and production in the Bay of Brest. If the sponge Si deposition was twice smaller than the sponge Si production yr after yr, it would mean that the sponge fauna of the Bay of Brest would be increasing at a rate of $92 \pm 241 \times 10^3$ kg Si yr^{-1} ($3.3 \pm 8.6 \times 10^6$ mol Si yr^{-1}), which would double the sponge Si standing stock (i.e., the sponge population) in about 13 yr. This disagrees with the data from our sponge fauna survey of

the Bay over the last 6 yr and the long-term survey conducted in the area by the Marine Observatory of the IUEM since 1997, which do not indicate that the sponge populations of the Bay are increasing at such high rate, rather the abundance and biomass of the sponge assemblages appear to be relatively constant in the long run (J. Grall pers. comm.). Some reasons may contribute to the imbalance between the annual silica production and deposition rates. First, the sponge mortality rate is unlikely to be constant every yr. Indeed, a longer time frame (of at least a decade) is likely needed to capture the Si cycling dynamics in the sponge populations (McMurray et al. 2015; Bell et al. 2017). Second, there might be some rapid (< 1 yr) dissolution of the most labile parts of the silica in the sponge spicules upon they are freed to the seafloor. Although sponge silica is more resistant to dissolution than that of other silicifiers (Rützler and Macintyre 1978; Erez et al. 1982; Maldonado et al. 2019), the most labile fraction of the sponge silica might be dissolved before the spicules being accumulated in the sediments. This would be in agreement with a recent study (Ng et al. 2020) that has measured through δ^{30} Si that the remineralization of silica from demosponges—the same Class of sponges as those occurring in the Bay of Brest—may be locally significant in surface sediments where sponges abound. In the study, Ng and co-authors determined that the benthic Si effluxes from bottoms with sponges were from 2 to 10 times higher than those from sediments without sponges. Finally, it cannot be excluded that part of the sponge silica deposited on the Bay bottoms is exported out of the Bay during the monthly strong tidal currents during spring tides or during extreme storms events, the force of which has been suggested to partially transport the deposited sediments of the Bay (Beudin 2014). Further research is necessary to resolve which of these processes, or if a combination of them, could explain the imbalance between the annual sponge silica production and deposition rates at the Bay. In particular, a long-term monitoring of the sponge fauna of the Bay will help to further understanding the functioning of the sponge Si dynamics in this ecosystem and to integrate long-term (> 1 yr) processes (e.g., mortality) into annual estimations of sponge Si. In addition, it would be interesting to investigate what the silica dissolution of the sponge species of the Bay represents, for which there is no information yet. This would provide a better understanding of the proportion of sponge skeletons (if any) that dissolves before the burial process begins.

Through deposition, the sponge silica accumulates in the sediments of the Bay and is finally buried at an average rate of 0.06 cm yr^{-1} (Gregoire et al. 2017; Ehrhold et al. 2021). Within the first centimeters of marine sediments, biogenic silica—no matter its origin—dissolves progressively until the interstitial water becomes saturated in dissolved Si, an asymptotic condition in which biogenic silica dissolution typically ceases (Rickert et al. 2002; Sarmiento and Gruber 2006; Khalil et al. 2007). In the sediments of the Bay of Brest, the

interstitial water reaches a dissolved Si asymptote at 10–15 cm burial depth (Raimonet et al. 2013), meaning that below that threshold, the amount of sponge silica buried annually ($57 \pm 18 \times 10^3$ kg Si yr⁻¹; Fig. 5) is preserved definitively in the sediments of the Bay. The difference between the sponge silica deposited in surface sediments and that buried definitively in the sediments ($51 \pm 18 \times 10^3$ kg Si yr⁻¹; Fig. 5) is assumed to be dissolved as interstitial dissolved Si during the early steps of burial. Such amount of dissolved Si contributes to the saturation of interstitial water and ultimately feeds the Si benthic efflux from the sediments of the Bay toward the water column, a recycling process that helps to sustain the populations of planktonic diatoms during the productive season in the Bay (Chauvaud et al. 2000; Ragueneau et al. 2002). Such amount might contribute about 5.4% of the total benthic Si flux of the Bay, which was estimated to be 1907 kg Si yr⁻¹ (Fig. 5; Ragueneau et al. 2005). Further investigation on the processes involved in the dissolution of sponge silica during the early steps of burial would help to quantify more accurately at which level the sponge Si contributes to the benthic dissolved Si efflux.

Sponge vs. diatom Si cycle at the Bay of Brest

The biogeochemical cycling of Si in the Bay of Brest through planktonic diatoms is well studied (Delmas and Tréguer, 1983; Del Amo et al. 1997; Chauvaud et al. 2000; Beucher et al. 2004) and summarized in Ragueneau et al. (2005). This budget was based on diatom Si flux rates and did not consider the sponge Si flux rates, nor the biogenic silica stocks of sponges and diatoms in the living communities and sediments.

To compare the contribution of diatoms and sponges to the Si budget of the Bay, the standing stocks and Si reservoirs in the form of diatom silica were determined from the literature. According to it, the standing stock of diatoms in the water column of the Bay ranges from 0.12 to 1.98 $\mu\text{mol Si L}^{-1}$ over the yr (Beucher et al. 2004). Unlike sponges, diatom cells have an ephemeral life of only days. Therefore, the silica standing crop of planktonic diatoms is known to change drastically from week to week and over seasons, depending on nutrient availability and hydrological conditions (Sarhou et al. 2005; Falkowski and Oliver 2007; Armbrust 2009). If the annual mean of diatom silica in the Bay ($0.9 \mu\text{mol Si L}^{-1}$; Beucher et al. 2004) is homogeneously extrapolated to the whole volume of the Bay of Brest (1.07×10^{12} L), an average diatom silica standing stock of 27×10^3 kg Si (1.0×10^6 mol Si) is obtained (Fig. 5). This figure integrates the seasonal variability occurring over the yr in the Bay, which range from a minimal value of 18×10^3 kg Si (0.6×10^6 mol Si) in winter to a maximum value of 36×10^3 kg Si (1.3×10^6 mol Si) in spring.

The fate of diatom silica in surface sediments is largely influenced by the active filter-feeding of mollusks in the Bay, which defecate Si-rich feces that facilitate the retention of

diatom silica at the sediment surface (Chauvaud et al. 2000; Ragueneau et al. 2002; Ragueneau et al. 2005). The content of diatom silica in the surface sediment of the Bay was determined from the analysis of 86 sediment samples from 43 stations across the Bay, which capture both the intra-annual variability (43 samples were sampled in winter and 43 in late summer) and the different depositional environments of the Bay (Song and Ragueneau 2007). It resulted in an average diatom silica reservoir in the surface sediments of the Bay of 248×10^3 kg Si (8.8×10^6 mol Si; Fig. 5).

When the Si stocks and fluxes of sponges are compared with those of planktonic diatoms, there are marked differences (Fig. 5). The rates at which Si is processed through diatoms are one order of magnitude higher than those through sponges. On the contrary, diatom Si stocks are between 7 and 45 times smaller than those of sponges (Fig. 5), in agreement with the only study to date comparing Si standing stocks in sponges and diatoms in a coastal ecosystem (Maldonado et al. 2010). These differences indicate that sponges and diatoms play their respective roles in the Si budget of the Bay at different speeds and through different mechanisms. The turnover of the diatom silica standing stock (i.e., standing stock: production rate) in the Bay is about 3 d, whereas that of sponge silica is about 6 yr, that is, approximately 800 times slower than that of diatom silica. Similarly, the turnover of diatom silica stock in surface sediments (i.e., reservoir in sediment: deposition rate) is about 1 month, whereas that of sponge silica is about 16 yr (ca. 170 times that of diatom silica). This means that the cycling of Si through diatoms is comparatively faster, with Si mainly cycling through them (repeatedly over a yr) rather than being accumulated. In contrast, Si accumulates in huge amounts in sponges over long periods (≥ 10 yr), being slowly processed through them. These results show that impacts on either the sponge populations or the sediments nearby sponge aggregations could have a long-term impact on the sponge Si cycling dynamics, which will require decades to be restored.

Conclusion

In shallow-water ecosystems, planktonic and benthic silicifiers have to share the dissolved Si pool and compete to incorporate this nutrient, which is critical for the growth of both organisms. Our study highlights that even in coastal, shallow-water systems with a high primary productivity dominated by planktonic diatoms—such as the Bay of Brest, sponges may account for a stock of biogenic silica as large as 89–98%. This stock cycles slowly compared to that of diatoms and accumulates biogenic Si in the sediments. These results suggest that the Si cycling through sponge communities is substantially different from that through diatom assemblages. Therefore, the comparison between the roles of these two groups of silicifiers is not straightforward due to their contrasting biological features (e.g., benthic and long living vs planktonic and short living). Yet these two types of silicifiers

need to be quantitatively integrated in future approaches, if we aim to understand the intricacies of the Si cycle in coastal systems.

Data availability statement

Data and metadata of this study are available at <http://hdl.handle.net/10261/275469>.

References

- Armbrust, E. V. 2009. The life of diatoms in the world's oceans. *Nature* **459**: 185–192. doi:10.1038/nature08057
- Ávila, E., and R. Riosmena-Rodríguez. 2011. A preliminary evaluation of shallow-water rhodolith beds in Bahía Magdalena, Mexico. *Braz. J. Oceanogr.* **59**: 365–375. doi:10.1590/S1679-87592011000400007
- Bavestrello, G., R. Cattaneo-Vietti, C. Cerrano, S. Cerutti, and M. Sarà. 1996. Contribution of sponge spicules to the composition of biogenic silica in the Ligurian Sea. *Mar. Ecol.* **17**: 41–50. doi:10.1111/j.1439-0485.1996.tb00488.x
- Bell, J. J., A. Biggerstaff, T. Bates, H. Bennett, J. Marlow, E. McGrath, and M. Shaffer. 2017. Sponge monitoring: Moving beyond diversity and abundance measures. *Ecol. Indic.* **78**: 470–488. doi:10.1016/j.ecolind.2017.03.001
- Beucher, C., P. Tréguer, R. Corvaisier, A. M. Hapette, and M. Elskens. 2004. Production and dissolution of biosilica, and changing microphytoplankton dominance in the Bay of Brest (France). *Mar. Ecol. Prog. Ser.* **267**: 57–69. doi:10.3354/meps267057
- Beudin, A. 2014. Dynamique et échanges sédimentaires en rade de Brest impactés par l'invasion de crépidules. Ph.D. thesis. Université de Bretagne Occidentale.
- Biard, T., J. W. Krause, M. R. Stukel, and M. D. Ohman. 2018. The significance of giant phaeodarians (Rhizaria) to biogenic silica export in the California Current Ecosystem. *Global Biogeochem. Cycl.* **32**: 987–1004. doi:10.1029/2018gb005877
- Chauvaud, L., F. Jean, O. Ragueneau, and G. Thouzeau. 2000. Long-term variation of the Bay of Brest ecosystem: Benthic-pelagic coupling revisited. *Mar. Ecol. Prog. Ser.* **200**: 35–48. doi:10.3354/meps200035
- Chou, Y., J. Y. Lou, C.-T. A. Chen, and L.-L. Liu. 2012. Spatial distribution of sponge spicules in sediments around Taiwan and the Sunda Shelf. *J. Oceanogr.* **68**: 905–912. doi:10.1007/s10872-012-0143-7
- Chu, J. W. F., M. Maldonado, G. Yahel, and S. P. Leys. 2011. Glass sponge reefs as a silicon sink. *Mar. Ecol. Prog. Ser.* **441**: 1–14. doi:10.3354/meps09381
- Davidson, K., R. J. Gowen, P. J. Harrison, L. E. Fleming, P. Hoagland, and G. Moschonas. 2014. Anthropogenic nutrients and harmful algae in coastal waters. *J. Environ. Manage.* **146**: 206–216. doi:10.1016/j.jenvman.2014.07.002
- Del Amo, Y., B. Quéguiner, P. Tréguer, H. Breton, and L. Lampert. 1997. Impacts of high-nitrate freshwater inputs on macrotidal ecosystems. II. Specific role of the silicic acid pump in the year-round dominance of diatoms in the Bay of Brest (France). *Mar. Ecol. Prog. Ser.* **161**: 225–237. doi:10.3354/meps161225
- Delmas, R., and P. Tréguer. 1985. Simulation de l'évolution de paramètres physiques, chimiques, et de la biomasse phyto-planctonique en période printanière dans un écosystème littoral macrotidal. *Oceanis* **11**: 197–211.
- DeMaster, D. J. 2003. The diagenesis of biogenic silica: Chemical transformations occurring in the water column, seabed, and crust, p. 87–98. *In* F. T. Mackenzie [ed.], *Treatise on geochemistry*. Elsevier.
- Derrien-Courtel, S., and others. 2019. Surveillance du benthos du littoral Breton. *Années 2017–2018 Rapport final*. Museum d'Histoire Naturelle de Paris.
- Eberhardt, L. L. 1978. Appraising variability in population studies. *J. Wildlife Manage.* **42**: 207. doi:10.2307/3800260
- Ehrhold, A., G. Gregoire, S. Sabine, G. Jouet, and P. Le Roy. 2016. Present-day sedimentation rates and evolution since the last maximum flooding surface event in the Bay of Brest (W-N France). *Proceedings of the American Geophysical Union, AGU, Fall Meeting 2016*.
- Ehrhold, A., and others. 2021. Fossil maerl beds as coastal indicators of late Holocene palaeo-environmental evolution in the Bay of Brest (Western France). *Palaeogeogr. Palaeoclimatol. Palaeoecol.* **577**: 110525. doi:10.1016/j.palaeo.2021.110525
- Erez, J., K. Takahashi, and S. Honjo. 1982. In-situ dissolution experiment of radiolaria in the central North Pacific Ocean. *Earth Planet. Sci. Lett.* **59**: 245–254. doi:10.1016/0012-821X(82)90129-7
- Falkowski, P. G., and M. J. Oliver. 2007. Mix and match: How climate selects phytoplankton. *Nat. Rev. Microbiol.* **5**: 813–819. doi:10.1038/nrmicro1751
- Glibert, P. M., and M. A. Burford. 2017. Globally changing nutrient loads and harmful algal blooms. Recent advances, new paradigms, and continuing challenges. *Oceanography* **30**: 58–69.
- Grall, J., and M. Glémarec. 1997. Biodiversity of maerl beds in Brittany: Functional approach and anthropogenic impacts. *Vie et Milieu* **47**: 339–349.
- Gregoire, G., A. Ehrhold, P. Le Roy, G. Jouet, and T. Garlan. 2016. Modern morpho-sedimentological patterns in a tide-dominated estuary system: The Bay of Brest (west Brittany, France). *J. Maps* **12**: 1152–1159. doi:10.1080/17445647.2016.1139514
- Gregoire, G., P. Le Roy, A. Ehrhold, G. Jouet, and T. Garlan. 2017. Control factors of Holocene sedimentary infilling in a semi-closed tidal estuarine-like system: The Bay of Brest (France). *Mar. Geol.* **385**: 84–100. doi:10.1016/j.margeo.2016.11.005
- Gutt, J., A. Bohmer, and W. Dimmler. 2013. Antarctic sponge spicule mats shape macrobenthic diversity and act as a silicon trap. *Mar. Ecol. Prog. Ser.* **480**: 57–71. doi:10.3354/meps10226

- Gutt, J., J. Arndt, C. Kraan, B. Dorschel, M. Schröder, A. Bracher, and D. Piepenburg. 2019. Benthic communities and their drivers: A spatial analysis off the Antarctic Peninsula. *Limnol. Oceanogr.* **64**: 2341–2357. doi:10.1002/lno.11187
- Hily, C., P. Potin, and J.-Y. Floch. 1992. Structure of subtidal algal assemblages on soft-bottom sediments: Fauna/flora interactions and role of disturbances in the Bay of Brest, France. *Mar. Ecol. Prog. Ser.* **85**: 115–130. doi:10.3354/meps085115
- Hooper, J. N. A. 2019. Sponges, p. 170–186. In P. A. Hutchings, M. Kingsford, and O. Hoegh-Guldberg [eds.], *The great barrier reef: Biology, environment and management*. CSIRO Publishing.
- Jean, F. 1994. Modélisation à l'état stable des transferts de carbone dans le réseau trophique benthique de la rade de Brest (France). Ph.D. thesis. Université de Bretagne Occidentale.
- Kersken, D., B. Feldmeyer, and D. Janussen. 2016. Sponge communities of the Antarctic peninsula: Influence of environmental variables on species composition and richness. *Polar Biol.* **39**: 851–862. doi:10.1007/s00300-015-1875-9
- Khalil, K., C. Rabouille, M. Gallinari, K. Soetaert, D. J. DeMaster, and O. Ragueneau. 2007. Constraining biogenic silica dissolution in marine sediments: A comparison between diagenetic models and experimental dissolution rates. *Mar. Chem.* **106**: 223–238. doi:10.1016/j.marchem.2006.12.004
- Kristiansen, S., and E. E. Hoell. 2002. The importance of silicon for marine production. *Hydrobiologia* **484**: 21–31. doi:10.1023/A:1021392618824
- Lambert, C., M. Vidal, A. Penaud, N. Combourieu-Nebout, V. Lebreton, O. Ragueneau, and G. Gregoire. 2017. Modern palynological record in the Bay of Brest (NW France): Signal calibration for palaeo-reconstructions. *Rev. Palaeobot. Palynol.* **244**: 13–25. doi:10.1016/j.revpalbo.2017.04.005
- Le Pape, O., Y. Del Amo, A. Menesguen, A. Aminot, B. Quéquiner, and P. Tréguer. 1996. Resistance of a coastal ecosystem to increasing eutrophic conditions: The Bay of Brest (France), a semi-enclosed zone of Western Europe. *Cont. Shelf Res.* **16**: 1885–1907. doi:10.1016/0278-4343(95)00068-2
- Llopis Monferrer, N., D. Boltovskoy, P. Tréguer, M. M. Sandin, F. Not, and A. Leynaert. 2020. Estimating biogenic silica production of Rhizaria in the global ocean. *Global Biogeochem. Cycl.* **34**. doi:10.1029/2019GB006286
- López-Acosta, M. 2022. Map of the benthic marine superhabitats of the Bay of Brest. INDIGEO. doi: 10.35110/7aa4a43a-e412-4021-9550-eb369a45fd42.
- López-Acosta, M., A. Leynaert, and M. Maldonado. 2016. Silicon consumption in two shallow-water sponges with contrasting biological features. *Limnol. Oceanogr.* **61**: 2139–2150. doi:10.1002/lno.10359
- López-Acosta, M., A. Leynaert, J. Grall, and M. Maldonado. 2018. Silicon consumption kinetics by marine sponges: An assessment of their role at the ecosystem level. *Limnol. Oceanogr.* **63**: 2508–2522. doi:10.1002/lno.10956
- Lukowiak, M., A. Pisera, and A. O'Dea. 2013. Do spicules in sediments reflect the living sponge community? A test in a Caribbean shallow-water lagoon. *PALAIOS* **28**: 373–385. doi:10.2110/palo.2012.p12-082r
- Maldonado, M., C. Carmona, Z. Velásquez, A. Puig, A. Cruzado, A. López, and C. M. Young. 2005. Siliceous sponges as a silicon sink: An overlooked aspect of benthopelagic coupling in the marine silicon cycle. *Limnol. Oceanogr.* **50**: 799–809. doi:10.4319/lo.2005.50.3.0799
- Maldonado, M., A. Riesgo, A. Bucci, and K. Rützler. 2010. Revisiting silicon budgets at a tropical continental shelf: Silica standing stocks in sponges surpass those in diatoms. *Limnol. Oceanogr.* **55**: 2001–2010. doi:10.4319/lo.2010.55.5.2001
- Maldonado, M., L. Navarro, A. Grasa, A. González, and I. Vaquerizo. 2011. Silicon uptake by sponges: A twist to understanding nutrient cycling on continental margins. *Sci. Rep.* **1**: 8. doi:10.1038/srep00030
- Maldonado, M., and others. 2017. Sponge grounds as key marine habitats: A synthetic review of types, structure, functional roles, and conservation concerns, p. 145–184. In S. Rossi, L. Bramanti, A. Gori, and C. Orejas Saco del Valle [eds.], *Marine animal forests: The ecology of benthic biodiversity hotspots*. Springer International Publishing.
- Maldonado, M., M. López-Acosta, C. Sitjà, M. García-Puig, C. Galobart, G. Erçilla, and A. Leynaert. 2019. Sponge skeletons as an important sink of silicon in the global oceans. *Nat. Geosci.* **12**: 815–822. doi:10.1038/s41561-019-0430-7
- Maldonado, M., L. Beazley, M. López-Acosta, E. Kenchington, B. Casault, U. Hanz, and F. Mienis. 2021. Massive silicon utilization facilitated by a benthic-pelagic coupled feedback sustains deep-sea sponge aggregations. *Limnol. Oceanogr.* **66**: 366–391. doi:10.1002/lno.11610
- Malviya, S., and others. 2016. Insights into global diatom distribution and diversity in the world's ocean. *Proc. Natl. Acad. Sci. USA* **113**: E1516–E1525. doi:10.1073/pnas.1509523113
- Masqué, P., E. Isla, J. A. Sanchez-Cabeza, A. Palanques, J. M. Bruach, P. Puig, and J. Guillén. 2002. Sediment accumulation rates and carbon fluxes to bottom sediments at the Western Bransfield Strait (Antarctica). *Deep-Sea Res. II Top. Stud. Oceanogr.* **49**: 921–933. doi:10.1016/S0967-0645(01)00131-X
- McGrath, E. C., L. Woods, J. Jompa, A. Haris, and J. J. Bell. 2018. Growth and longevity in giant barrel sponges: Redwoods of the reef or pines in the Indo-Pacific? *Sci. Rep.* **8**: 15317. doi:10.1038/s41598-018-33294-1
- McMurray, S. E., J. E. Blum, and J. R. Pawlik. 2008. Redwood of the reef: Growth and age of the giant barrel sponge

- Xestospongia muta* in the Florida keys. *Mar. Biol.* **155**: 159–171. doi:10.1007/s00227-008-1014-z
- McMurray, S. E., C. M. Finelli, and J. R. Pawlik. 2015. Population dynamics of giant barrel sponges on Florida coral reefs. *J. Exp. Mar. Biol. Ecol.* **473**: 73–80. doi:10.1016/j.jembe.2015.08.007
- Neill, K. F., W. A. Nelson, R. D'Archino, D. Leduc, and T. J. Farr. 2015. Northern New Zealand rhodoliths: Assessing faunal and floral diversity in physically contrasting beds. *Mar. Biodivers.* **45**: 63–75. doi:10.1007/s12526-014-0229-0
- Ng, H. C., L. Cassarino, R. A. Pickering, E. M. S. Woodward, S. J. Hammond, and K. R. Hendry. 2020. Sediment efflux of silicon on the Greenland margin and implications for the marine silicon cycle. *Earth Planet. Sci. Lett.* **529**: 115877. doi:10.1016/j.epsl.2019.115877
- QGIS Development Team. 2020. QGIS geographic information system. Project.
- Quéguiner, B., and P. Tréguer. 1984. Studies on the phytoplankton in the Bay of Brest (western Europe). Seasonal variations in composition, biomass and production in relation to hydrological and chemical features (1981–1982). *Bot. Mar.* **27**: 449–459. doi:10.1515/botm.1984.27.10.449
- Ragueneau, O., and others. 2002. Direct evidence of a biologically active coastal silicate pump: Ecological implications. *Limnol. Oceanogr.* **47**: 1849–1854. doi:10.4319/lo.2002.47.6.1849
- Ragueneau, O., L. Chauvaud, B. Moriceau, A. Leynaert, G. Thouzeau, A. Donval, F. Le Loc'h, and F. Jean. 2005. Biodeposition by an invasive suspension feeder impacts the biogeochemical cycle of Si in a coastal ecosystem (Bay of Brest, France). *Biogeochemistry* **75**: 19–41. doi:10.1007/s10533-004-5677-3
- Ragueneau, O., D. J. Conley, A. Leynaert, S. N. Longphuir, and C. P. Slomp. 2006. Role of diatoms in silica cycling and coastal marine food webs, p. 163–195. *In* V. Ittekkot, D. Unger, C. Humborg, and N. T. An [eds.], *The silicon cycle: Human perturbations and impacts on aquatic systems*. Island Press.
- Ragueneau, O., and others. 2018. The impossible sustainability of the Bay of Brest? Fifty years of ecosystem changes, interdisciplinary knowledge construction and key questions at the science-policy-community interface. *Front. Mar. Sci.* **5**: 124. doi:10.3389/fmars.2018.00124
- Raimonet, M., O. Ragueneau, F. Andrieux-Loyer, X. Philippon, R. Kerouel, M. Le Goff, and L. Mémery. 2013. Spatio-temporal variability in benthic silica cycling in two macrotidal estuaries: Causes and consequences for local to global studies. *Estuar. Coast. Shelf Sci.* **119**: 31–43. doi:10.1016/j.ecss.2012.12.008
- Reincke, T., and D. Barthel. 1997. Silica uptake kinetics of *Halichondria panicea* in Kiel Bight. *Mar. Biol.* **129**: 591–593. doi:10.1007/s002270050200
- Rickert, D., M. Schlüter, and K. Wallmann. 2002. Dissolution kinetics of biogenic silica from the water column to the sediments. *Geochim. Cosmochim. Acta* **66**: 439–455. doi:10.1016/S0016-7037(01)00757-8
- Ríos, P., and J. Cristobo. 2014. Antarctic Porifera database from the Spanish benthic expeditions. *ZooKeys* **401**: 1–10. doi:10.3897/zookeys.401.5522
- Rützler, K., and I. G. Macintyre. 1978. Siliceous sponge spicules in coral-reef sediments. *Mar. Biol.* **49**: 147–159. doi:10.1007/bf00387114
- Salomon, J. C., and M. Breton. 1991. Numerical study of the dispersive capacity of the Bay of Brest, France, towards dissolved substances, p. 459–464. *In* *Environmental hydraulics*, Balkema, Rotterdam (The Netherlands).
- Sandford, F. 2003. Physical and chemical analysis of the siliceous skeletons in six sponges of two groups (Demospongiae and Hexactinellida). *Microsc. Res. Tech.* **62**: 336–355. doi:10.1002/jemt.10400
- Sañé, E., E. Isla, M. Á. Bárcena, and D. J. DeMaster. 2013. A shift in the biogenic silica of sediment in the Larsen B continental shelf, off the Eastern Antarctic Peninsula, resulting from climate change. *PLoS One* **8**: e52632. doi:10.1371/journal.pone.0052632
- Sarmiento, J., and N. Gruber. 2006. *Ocean biogeochemical dynamics*. Princeton Univ. Press.
- Sarthou, G., K. R. Timmermans, S. Blain, and P. Tréguer. 2005. Growth physiology and fate of diatoms in the ocean: A review. *J. Sea Res.* **53**: 25–42. doi:10.1016/j.seares.2004.01.007
- Sciberras, M., M. Rizzo, J. R. Mifsud, K. Camilleri, J. A. Borg, E. Lanfranco, and P. J. Schembri. 2009. Habitat structure and biological characteristics of a maerl bed off the northeastern coast of the Maltese Islands (central Mediterranean). *Mar. Biodiv.* **39**: 251–264. doi:10.1007/s12526-009-0017-4
- Song, Y. P., and O. Ragueneau. 2007. Le dosage de bSiO₂ dans le sédiment de la rade de Brest. Master thesis. Université de Bretagne Occidentale.
- Teixidó, N., J. Garrabou, and J.-G. Harmelin. 2011. Low dynamics, high longevity and persistence of sessile structural species dwelling on Mediterranean coralligenous outcrops. *PLoS One* **6**: e23744. doi:10.1371/journal.pone.0023744
- Thorel, M., and others. 2017. Nutrient ratios influence variability in *Pseudo-nitzschia* species diversity and particulate domoic acid production in the Bay of Seine (France). *Harmful Algae* **68**: 192–205. doi:10.1016/j.hal.2017.07.005
- Tréguer, P. J., and others. 2021. Reviews and syntheses: The biogeochemical cycle of silicon in the modern ocean. *Biogeosciences* **18**: 1269–1289. doi:10.5194/bg-18-1269-2021
- Van Soest, R. W. M., and others. 2012. Global diversity of sponges (Porifera). *PLoS One* **7**: e35105. doi:10.1371/journal.pone.0035105

Acknowledgments

The authors thank Erwan Amice, Isabelle Bihannic, and Thierry Le Bec for assistance during underwater fieldwork and for pictures of Fig. 1c–g.

Marta García Puig and Marcos Navas Durán are thanked for helping with the data management of spicule counting. The authors also thank the staff maintaining the SOMLIT-Lanvéoc database for making public their information on nutrient availability at the bottom waters of the Bay of Brest, and Sébastien Hervé and Natalia Llopis Monferrer for their help with the artwork of Fig. 5. Jill Sutton is especially thanked for her comments on the manuscript. The authors also thank two anonymous referees for their comments during the review of this manuscript. This research was supported by two Spanish Ministry grants (CTM2015-67221-R and MICIU: #PID2019-108627RB-I00) to M.M., the French National Research Program EC2CO (12735—AO2020) to J.G., and the ISblue Project, Interdisciplinary Graduate School for the Blue Planet (ANR-17-EURE-0015), co-funded by a grant from the French government under the program

“Investissements d’Avenir,” to M.L.A. M.L.A. thanks the Xunta de Galicia for her postdoctoral grant (IN606B-2019/002), which also supported this work.

Conflict of Interest

None declared.

Submitted 22 October 2021

Revised 18 July 2022

Accepted 11 August 2022

Associate editor: Robinson W. Fulweiler